SHELL MODEL AND SPECTROSCOPIC FACTORS

ALFREDO POVES

Departamento de Física Teórica,
Universidad Autónoma de Madrid and IFT,
UAM/CSIC, E-28049, Madrid, Spain

Résumé

Dans ce cours, on introduit la notion de facteur spectroscopique dans le contexte du modèle en couches du noyau. On donne aussi une introduction aux développements récents des calculs à grande échelle du Modèle en Couches en Interaction. Finalement, les facteurs spectroscopiques et les fragmentations des états sont discutés pour des noyaux sphériques proches des fermetures de couches mágiques ainsi que pour des noyaux deformés.

Abstract

In these lectures, I introduce the notion of spectroscopic factor in the shell model context. A brief review is given of the present status of the large scale applications of the Interacting Shell Model. The spectroscopic factors and the spectroscopic strength are discussed for nuclei in the vicinity of magic closures and for deformed nuclei.

Contents

1 Introduction

The basic idea of the Independent Particle Model (IPM) is to assume that, at zeroth order, the result of the complicated two body interactions among the nucleons is to produce an average self-binding potential. Mayer and Jensen (1949) [1] proposed an spherical mean field consisting in an isotropic harmonic oscillator plus a strongly attractive spin-orbit potential and an orbit-orbit term. Later, other functional forms were adopted, *e.g.* the Woods-Saxon well. The usual procedure to generate a mean field in a system of N interacting fermions, starting from their free interaction, is the Hartree-Fock approximation, extremely successful in atomic physics. Whatever the origin of the mean field, the eigenstates of the N-body problem are Slater determinants *i.e.* anti-symmetrized products of N single particle wave functions. In the nucleus, there is a catch, because the very strong short range repulsion and the tensor force make the HF approximation based upon the bare nucleon-nucleon force impracticable. However, at low energy, the nucleus do manifest itself as a system of independent particles in many cases, and when it does not, it is due to the medium range correlations that produce strong configuration mixing and not to the short range repulsion.

Does the success of the shell model really "prove" that nucleons move independently in a fully occupied Fermi sea as assumed in HF approaches? In fact, the single particle motion can persist at low energies in fermion systems due to the suppression of collisions by Pauli exclusion (Pandharipande et al., [2]).

Brueckner theory takes advantage of the Pauli blocking to regularize the bare nucleon- nucleon interaction, in the form of density dependent effective interactions of use in HF calculations or G-matrices for large scale shell model calculations.

The wave function of the ground state of a nucleus in the IPM is the product of an Slater determinant for the Z protons that occupy the Z lowest states in the mean field and another Slater determinant for the N neutrons in the N lowest states of the mean field. In second quantization, this state can be written as:

$$|N\rangle \cdot |Z\rangle \qquad \text{with:} \tag{1}$$

$$|N\rangle = n_1^\dagger n_2^\dagger \dots n_N^\dagger |0\rangle \tag{2}$$

$$|Z\rangle = z_1^\dagger z_2^\dagger \dots z_Z^\dagger |0\rangle \tag{3}$$

It is obvious that the occupied states have occupation number 1 and the empty ones occupation number 0.

1.1 Spectroscopic factors.

Lets denote the nucleon creation and annihilation operators by $a^\dagger$ and a, and consider the ground states of the systems of A-1, A, and A+1 nucleons, then,

$$|A\rangle = a_1^\dagger a_2^\dagger \dots a_A^\dagger |0\rangle \qquad \text{and, trivially} \tag{4}$$

$$\langle A+1|a_{A+1}^\dagger|A\rangle = 1 \;\; ; \;\; \langle A+1|a_{\neq A+1)}^\dagger|A\rangle = 0 \tag{5}$$

$$\langle A-1|a_{A-1}|A\rangle = 1 \;\; ; \;\; \langle A-1|a_{\neq A-1)}|A\rangle = 0. \tag{6}$$

The expectation values of the operators $a^\dagger$ and a between the states of the nuclei with A+1 and A, and A-1 and A, give the spectroscopic amplitudes for stripping and pick-up reactions. The spectroscopic factors are the squares of this amplitudes with some angular momentum coefficients. When correlations are included, the spectroscopic amplitudes depart from their 0 or 1 values. The knowledge of the spectroscopic factors make it possible to learn about the structure of the mean field and the role of correlations.

1.2 Spectroscopic Factors and the Meaning of the Shell Model.

The nuclear correlations modify the IPM picture. In Figure 1 we show the results of the Correlated Basis Function calculation of Fantoni and Pandharipande [3] for nuclear matter. If we had a system of non interacting fermions, the figure would be just a step function corresponding to occupation 1 below the Fermi level and occupation 0 above.

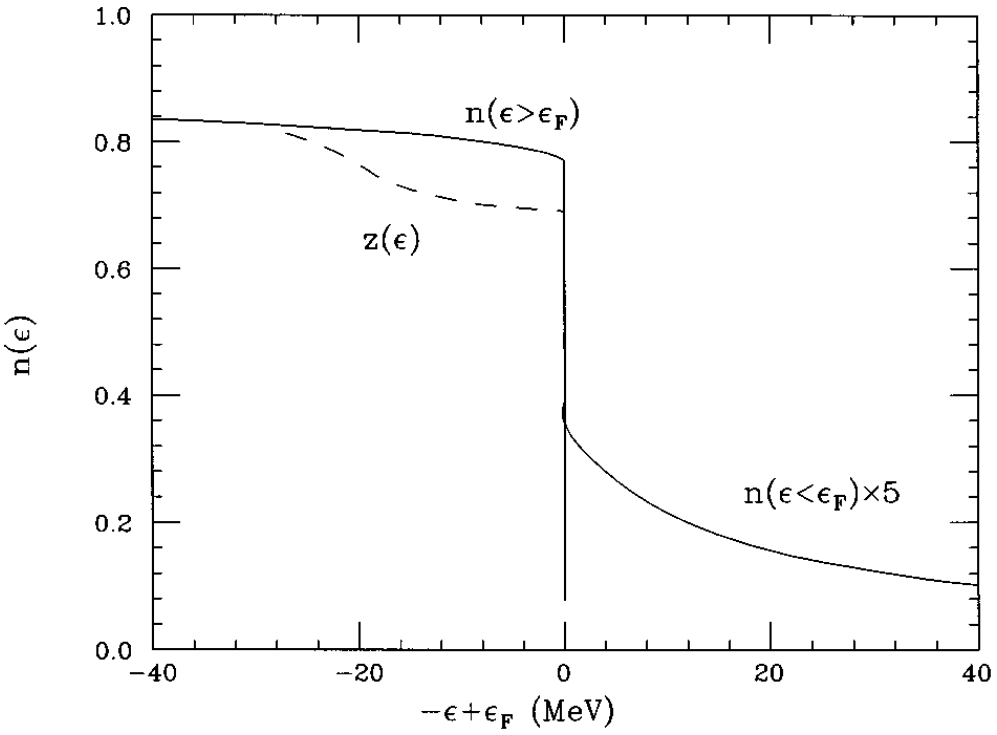

Figure 1: Dilution of the Spectroscopic strength by the bare N-N interaction. Results for nuclear matter. Figure borrowed from ref. [2]

In spite of that, the nuclear quasi-particles resemble extraordinarily to the mean field solutions of the IPM, as can be seen in the classical example of the charge density difference between ^{206}Pb and ^{205}Tl, measured in the electron scattering experiments of Cavedon *et al* [4] (Fig. 2) The shape of the $3s_{1/2}$ orbit is very well given by the mean field calculation. To make the agreement quantitative the density has to be calculated with the occupation numbers scaled down by a factor $\sim$0.7. To know more, read the article " Independent

particle motion and correlations in fermion systems" V. R. Pandharipande, I. Sick and P. K. A. deWitt Huberts, [2].

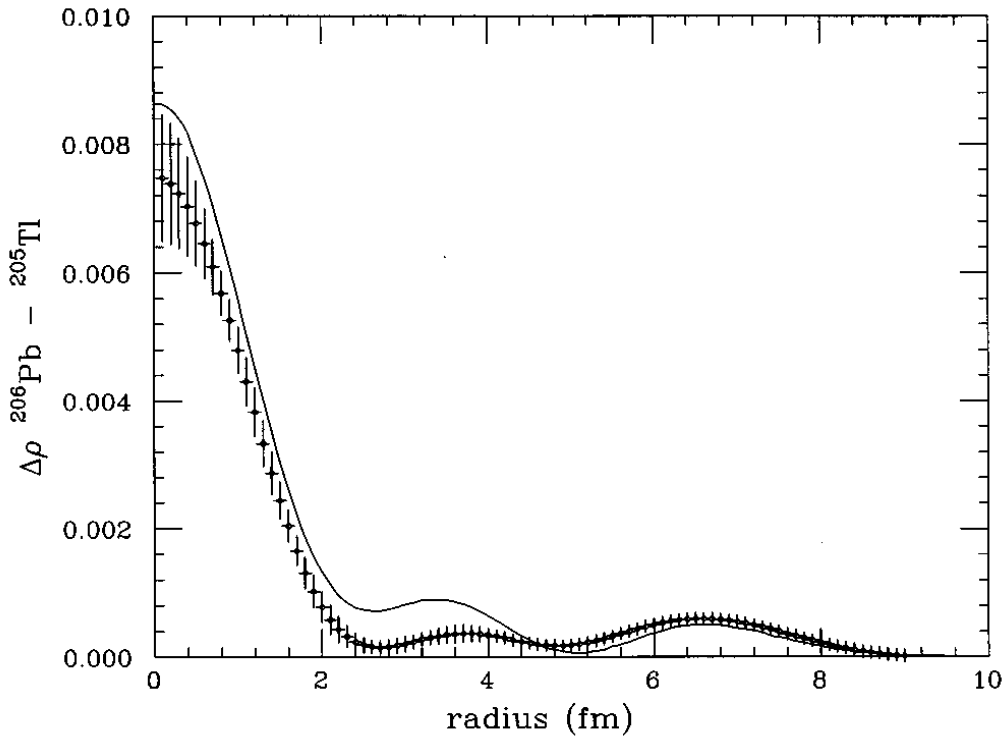

Figure 2: Charge density difference between ^{206}Pb and ^{205}Tl. Experiment vs. mean field calculation. Figure borrowed from ref. [2]

2 The Interacting Shell Model (ISM)

The ISM is an approximation to the exact solution of the nuclear A-body problem using effective interactions in restricted valence spaces. The effective interactions are obtained from the bare nucleon-nucleon interaction by means of a regularization procedure aimed to soften the short range repulsion. In other words, using effective interactions we can treat the A-nucleon system in a basis of independent quasi-particles. A Shell Model calculation amounts to diagonalizing the nuclear hamiltonian in the basis of all the Slater determinants that can be built distributing the valence particles in a set of orbits which is called valence space. The orbits that are always full form the core. The three pillars of the shell model are the effective interactions,

the valence spaces, and the algorithms and codes that make it possible to solve the secular problem. For a recent review of the ISM see; E. Caurier, G. Martínez-Pinedo, F. Nowacki, A. Poves and A. P. Zuker. "The Shell Model as a Unified View of Nuclear Structure", [5].

2.1 Making the Effective Interaction Simple.

The effective shell model interactions appear sometimes as a long list of meanigless numbers; the two body matrix elements of the Hamiltonian. Without loosing the simplicity of the Fock space representation, we can recast these numbers in a way full of physical insight, following Dufour-Zuker rules: *Any effective interaction can be split in two parts:* $\mathcal{H} = \mathcal{H}_m$*(monopole)* + $\mathcal{H}_M$*(multipole).* $\mathcal{H}_m$ *contains all the terms that are affected by a spherical Hartree-Fock variation, hence it is responsible for the global saturation properties and for the evolution of the spherical single particle energies* [6].

The Monopole Hamiltonian can be written as:

$$\mathcal{H}_m = H_{sp} + \sum \left[\frac{1}{(1+\delta_{ij})} a_{ij}\, n_i (n_j - \delta_{ij}) \right. \tag{7}$$

$$\left. + \frac{1}{2} b_{ij} \left(T_i \cdot T_j - \frac{3 n_i}{4} \delta_{ij} \right) \right].$$

The coefficients a and b are defined in terms of the centroïds:

$$V_{ij}^{T} = \frac{\sum_J V_{ijij}^{JT}[J]}{\sum_J [J]} \tag{8}$$

as: $a_{ij} = \frac{1}{4}(3V_{ij}^1 + V_{ij}^0)$, $b_{ij} = V_{ij}^1 - V_{ij}^0$, the sums run over Pauli allowed values.

The evolution of effective spherical single particle energies with the number of particles in the valence space is dictated by $\mathcal{H}_m$. In the case of identical particles the expression reads:

$$\epsilon_j(n) = \epsilon_j(n=1) + \sum_i V_{ij}^1 n_i \tag{9}$$

The monopole hamiltonian $\mathcal{H}_m$ also governs the relative position of the various T-values in the same nucleus, via the terms:

$$b_{ij} \;\; T_i \cdot T_j \tag{10}$$

Even small defects in the centroids can produce large changes in the relative position of the different configurations due to the appearance of

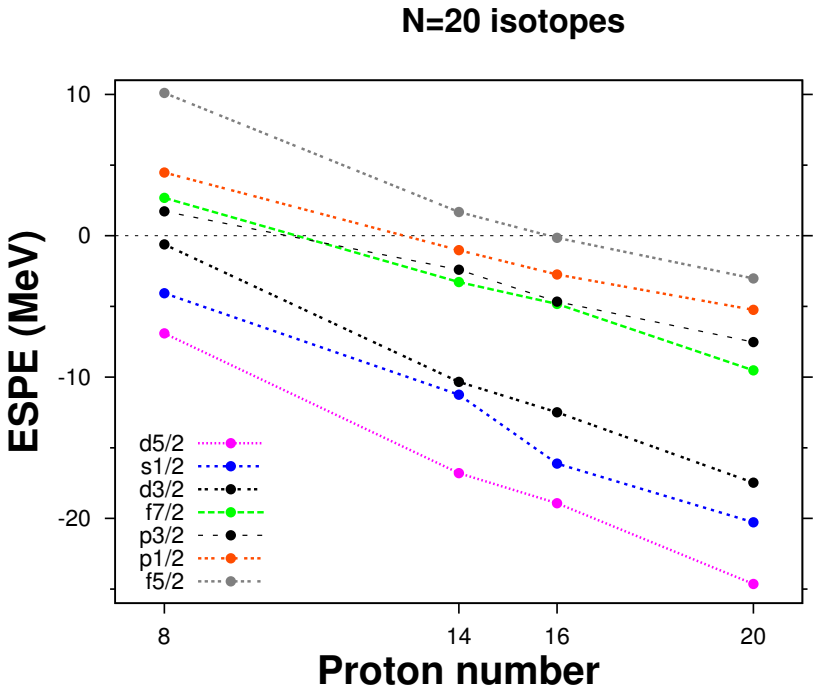

Figure 3: Effective single particle energies for the N=20 isotones from Oxygen to Calcium

quadratic terms involving the number of particles in the different orbits. These quadratic terms make it possible that deformed or superdeformed states of n-particles n-holes nature could appear at very low excitation energy in doubly magic nuclei as ^{16}O or ^{40}Ca.

The drift of the effective single particle energies is illustrated in Figure 3 for the N=20 isotones from Oxygen to Calcium. It is seen that, as we move far from stability, the effective gap between the *sd* and *pf* shells diminishes, and the $0f_{7/2}$ and $1p_{3/2}$ orbits change their ordering. Both facts contribute to the appearance of a region of deformation around ^{31}Na.

2.2 The Multipole Hamiltonian.

$\mathcal{H}_M$ can be written in two representations, particle-particle and particle-hole:

$$\mathcal{H}_M = \sum_{r\leq s,t\leq u,\Gamma} W^{\Gamma}_{rstu} Z^{+}_{rs\Gamma} \cdot Z_{tu\Gamma}, \tag{11}$$

$$\mathcal{H}_M = \sum_{rstu\Gamma} [\gamma]^{1/2} \frac{(1+\delta_{rs})^{1/2}(1+\delta_{tu})^{1/2}}{4} \omega^{\gamma}_{rtsu} (S^{\gamma}_{rt} S^{\gamma}_{su})^0, \tag{12}$$

where Z^{+}_{Γ} (Z_{Γ}) is the coupled product of two creation (annihilation)

operators and S^γ is the coupled product of one creation and one annihilation operator.

$$Z^+_{rs\Gamma} = [a^\dagger_r a^\dagger_s]^\Gamma \tag{13}$$

$$S^\gamma_{rs} = [a^\dagger_r a_s]^\gamma \tag{14}$$

The W and ω matrix elements are related by a Racah transformation:

$$\omega^\gamma_{rtsu} = \sum_\Gamma (-)^{s+t-\gamma-\Gamma} \left\{ \begin{array}{ccc} r & s & \Gamma \\ u & t & \gamma \end{array} \right\} W^\Gamma_{rstu}[\Gamma], \tag{15}$$

$$W^\Gamma_{rstu} = \sum_\gamma (-)^{s+t-\gamma-\Gamma} \left\{ \begin{array}{ccc} r & s & \Gamma \\ u & t & \gamma \end{array} \right\} \omega^\gamma_{rtsu}[\gamma]. \tag{16}$$

The operators $S^{\gamma=0}_{rr}$ are just the number operators for orbits r and $S^{\gamma=0}_{rr'}$ the spherical HF particle hole vertices. Both must have null coefficients if the monopole hamiltonian satisfies HF self-consistency. The operator $Z^+_{rr\Gamma=0}$ creates a pair of particles coupled to J=0 (or coupled to L=0 and S=0, or in a state of zero total momentum). Therefore the terms, $Z^+_{rr\Gamma=0} \cdot Z_{ss\Gamma=0}$ represent different pairing hamiltonians, whose specificities determine the values of the matrix elements $W^{\Gamma=0}_{rrss}$.

The operators S^γ_{rs} are typical multipole vertices of multipolarity γ. For instance, $r = s$, γ=(L=0,S=1) produces a $(\vec{\sigma}\cdot\vec{\sigma})$ term which is the main component of the residual interaction in He-3 droplets. The terms S^γ_{rs} γ=(J=2,T=0), which appear in the $(Q \cdot Q)$ interaction that is responsible for the existence of deformed nuclei, are specially large and attractive when $j_r - j_s$=2 and $l_r - l_s$=2.

A detailed analysis of the effective nucleon-nucleon interaction in the nucleus, using the techniques of ref. [6] reveals that the multipole hamiltonian is universal and dominated by BCS-like isovector and isoscalar pairing plus quadrupole-quadrupole and octupole-octupole terms of very simple nature $(r^\lambda Y_\lambda \cdot r^\lambda Y_\lambda)$, as can be seen in table I.

In summary, the key aspects of the effective interaction(s) are: a) The evolution of the spherical mean field in the valence spaces. In order to reproduce the experimental behavior, the present two body effective interactions, probably require to be complemented by three body forces whose need seems already well established by the Green Function Monte Carlo calculations [7] and No Core Shell model Calculations [8]. Some claim that they could be reducible to simple monopole forms, a kind of density dependence, or more precisely, occupation number dependence. and, b) The multipole hamiltonian – which drives the correlations – and which does not seem to demand

Table 1: Dominant terms of the multipole Hamiltonian for several pf-shell effective interactions

Interaction	particle-particle		particle-hole		
	JT=01	JT=10	$\lambda\tau$=20	$\lambda\tau$=40	$\lambda\tau$=11
KB3	-4.75	-4.46	-2.79	-1.39	+2.46
FPD6	-5.06	-5.08	-3.11	-1.67	+3.17
GOGNY	-4.07	-5.74	-3.23	-1.77	+2.46
GXPF1	-4.18	-5.07	-2.92	-1.39	+2.47
BONNC	-4.20	-5.60	-3.33	-1.29	+2.70

major changes with respect to the one derived from the realistic nucleon-nucleon potentials.

2.3 Collectivity in Nuclei.

The widespread presence of nuclei with deformed shapes is a conspicuous manifestation of the importance of the quadrupole-quadrupole terms in the nuclear multipole hamiltonian. Nuclear superfluidity (and the shift of the mass parabolas in even isobaric multiplets, and many other effects) signal also the importance of the pairing terms. For a given interaction, a many body system would or would not display coherent features at low energy depending on the structure of the mean field around the Fermi level. An attractive pairing interaction in an electron gas at T=0 produces the superconducting phase transition. The quadrupole-quadrupole interaction left alone –*i.e.*– if the monopole hamiltonian is negligible, would produce nuclear needles. Magic nuclei are spherical despite the strong quadrupole-quadrupole interaction, because the large gaps in the nuclear mean field at the Fermi surface block the quadrupole correlations. The isotropic harmonic oscillator has SU(3) symmetry. The quadrupole operators are generators of this group and the Casimir of the group contains the quadrupole-quadrupole interactions. Therefore the states of lower energy are those with maximal deformation compatible with the Pauli principle. The spin orbit interaction breaks the SU(3) symmetry, but other SU3 variants emerge when there are favorable orbits around the Fermi level, like Pseudo-SU3 or Quasi-SU3.

3 Spectroscopic factors

The spectroscopic factors are defined as:

$$S(j,t_z) = \frac{\langle J_f T_f T_{zf} || a^\dagger_{jt_z} || J_i T_i T_{zi} \rangle^2}{2J_f + 1} \tag{17}$$

where the matrix element is reduced in angular momentum only; j and t_z refer to the total angular momentum and third isospin component of the stripped nucleon. Imagine we start on doubly magic ^{48}Ca. The states

$$|r_{jt_z}\rangle = a^\dagger_{jt_z}|^{48}\text{Ca gs}\rangle \tag{18}$$

are not, except in the non-interacting case, eigenstates of the Hamiltonian for ^{49}Sc or ^{49}Ca. The stronger the correlations, the farther they are. Therefore, to calculate $S(j,t_z)$ we overlap $|r\rangle$ with the physical states in the final nucleus. In practice, we just take $|r\rangle$ as starting vector for a sequence of Lanczos iterations. The total spectroscopic factor is the norm of the state $|r\rangle$. The excitation energies of the starting vectors, $e_r = \langle r|H|r\rangle - \langle f|H|f\rangle$:

$$e_{p_{3/2}} = 4.54\ MeV \quad e_{p_{1/2}} = 5.99\ MeV \quad e_{f_{5/2}} = 5.76\ MeV$$

are almost identical to the monopole prediction:

$$\epsilon_{p_{3/2}} = 4.58\ MeV \quad \epsilon_{p_{1/2}} = 5.99\ MeV \quad \epsilon_{f_{5/2}} = 5.66\ MeV$$

a result readily explained by the weakness of the ground state correlations in ^{48}Ca. By the same token the sum rules for $(2j+1)S(j,t_z)$ are very close to their theoretical maximum, $(2j+1)$. Indeed, the sum rule is actually quenched by a factor of about 0.7 because of the short range correlations that take part of the wave function out of the model space.

3.1 Stripping on ^{48}Ca $\rightarrow$ ^{49}Sc

We have compared the experimentally available information with large scale shell model calculations in the full pf-shell using the interaction KB3 in ref. [9]. The spectroscopic factors for $f_{7/2}$ in Fig. 4, show little fragmentation.

For $p_{3/2}$, Fig. 5 seems to indicate a discrepancy between theory—that produces substantial fragmentation—and experiment, that falls quite short of the sum rule, by detecting basically only two peaks. Note that the higher, at around 11.5 MeV, corresponds to the IAS of the ground state of ^{49}Ca.

The discrepancy is explained when we consider Fig. 6 for the $p_{1/2}$ strength: now the too numerous experimental fragments abundantly exceed the sum rule. What seems to be happening is that the method chosen to analyse the data does not distinguish among the $L = 1$ peaks those with $J = 1/2$

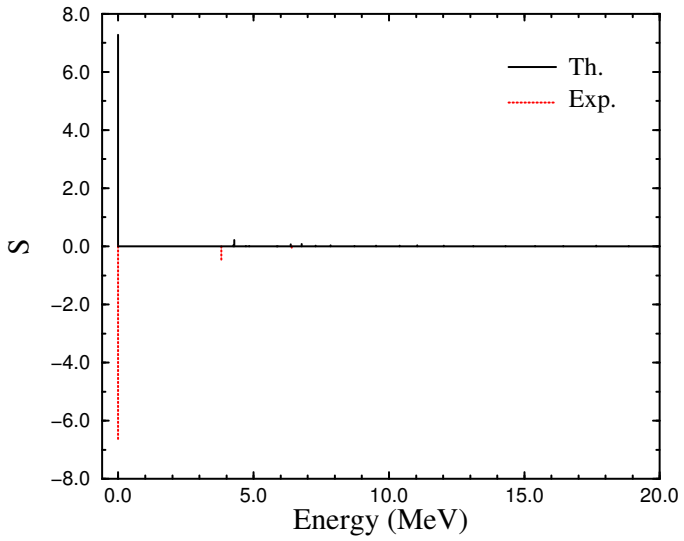

Figure 4: Stripping on ^{48}Ca $\rightarrow$ ^{49}Sc. $0f_{7/2}$ spectroscopic strength.

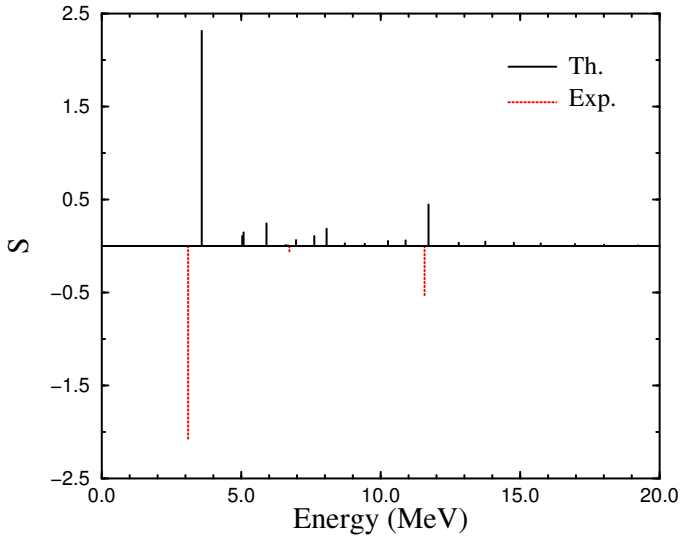

Figure 5: Stripping on ^{48}Ca $\rightarrow$ ^{49}Sc. $1p_{3/2}$ spectroscopic strength.

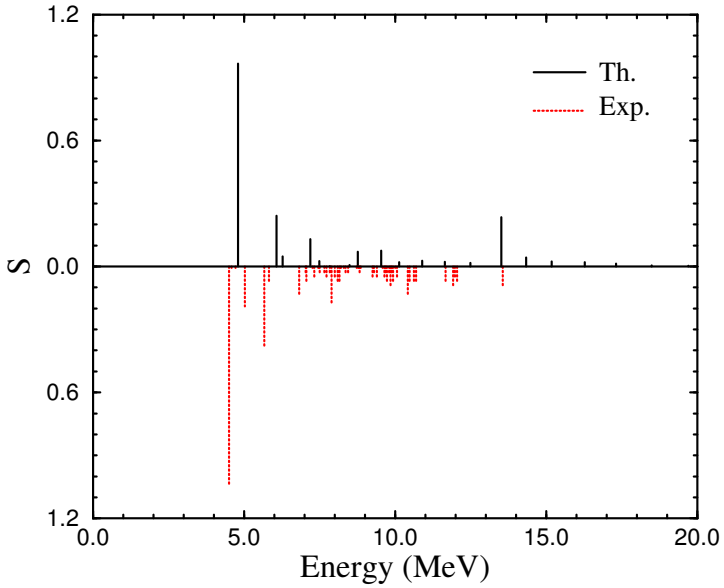

Figure 6: Stripping on ^{48}Ca $\rightarrow$ ^{49}Sc. $1p_{1/2}$ spectroscopic strength.

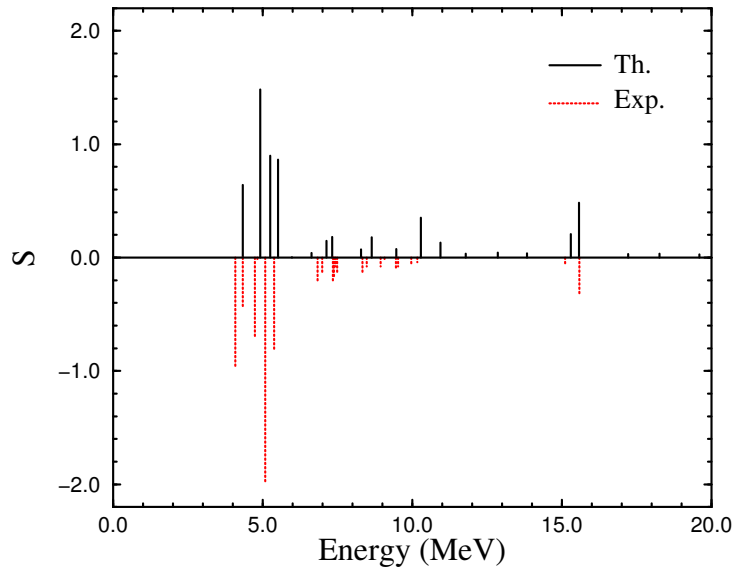

Figure 7: Stripping on ^{48}Ca $\rightarrow$ ^{49}Sc. $0f_{5/2}$ spectroscopic strength.

from those with $J = 3/2$, unduly favouring the former. Note that the lowest calculated state is a bit too high in Fig. 6. (The higher states are again isobaric analogues.)

The situation becomes truly satisfactory for the $f_{5/2}$ strength in Fig. 7. The four lowest theoretical peaks may demand a slight downward shift but they have nearly perfect counterparts in experiment, where a fifth state also shows—a probable intruder. Higher up the agreement remains quite good, especially if we remember that, at 60 iterations, the spikes beyond 7 MeV do not represent converged eigenstates but doorways, subject to further fragmentation. Note that it is the second of the two IAS levels slightly above 15 MeV that carries most of the strength.

3.2 Spectroscopic factors and correlations; ^{48}Ca *vs* ^{46}Ar

The correlations act in two ways: Shifting strength from the particle to the hole channel and fragmenting the strength into many states. For the neutron stripping on ^{48}Ca and ^{46}Ar [11] the situation is as follows:

- orbit strength
- f7/2 0.025(Ca) 0.136(Ar)
- p3/2 0.982(Ca) 0.793(Ar)
- p1/2 0.987(Ca) 0.966(Ar)
- f5/2 0.984(Ca) 0.969(Ar)

In the presence of correlations, when the single particle strength is fragmented, one can still have an idea of the bearings of the underlying mean field, constructing equivalent single particle energies [10].

$$\epsilon_j = \frac{\sum_n (E_0 - E_n^-) S_n^- + \sum_m (2j+1)(E_0 - E_m^+) S_m^+}{(2j+1)} \tag{19}$$

$$\sum_n S_n^- + (2j+1) \sum_m S_m^+ = 2j+1 \tag{20}$$

A recent discussion on this issue can be found in references [12, 13].

3.3 Deformed nuclei; Stripping on ^{48}Cr $\rightarrow$ ^{49}Cr

In deformed nuclei, much of the particle strength goes to the hole channel. We have made full pf-shell calculations with the KB3 interactions for the the spectroscopic factors of the stripping reaction ^{48}Cr $\rightarrow$ ^{49}Cr. Both nuclei are deformed with β $\sim$0.3. For instance in ^{48}Cr we have only 0.585 of $0f_{7/2}$ strength instead of 1.0 in the single particle limit. In addition the particle strength is fragmented among several states as can be seen in Fig.8. The lowest $7/2^-$ state in the figure belongs to the K=5/2 ground state band of ^{49}Cr and is located at $\sim$300 keV of excitation energy.

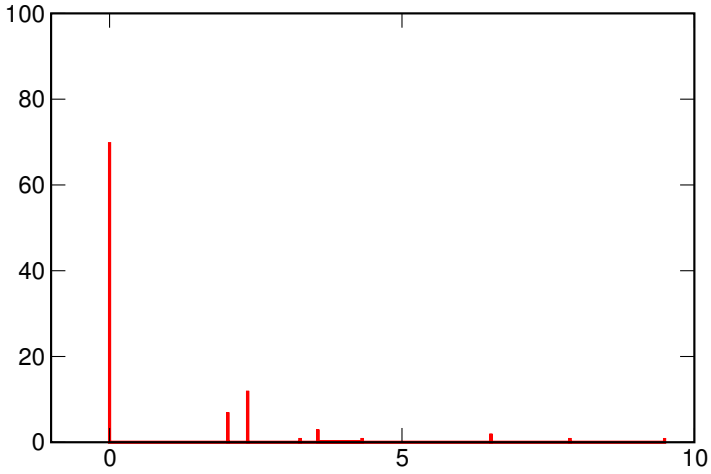

Figure 8: Stripping on ^{48}Cr $\rightarrow$ ^{49}Cr; $0f_{7/2}$ spectroscopic strength.

Most of the $0f_{5/2}$ strength (0.96) remains in the particle channel. But now the fragmentation, shown in Fig.9 is much stronger. It is interesting to realize that the ground state $J^\pi = 5/2^-$ does not have any $0f_{5/2}$ strength. This is an extreme –and very illustrative– example of a physical situation in which the correlations wash out completely the connection between the quantum numbers of one state and its spectroscopic strength for the orbit carrying the same quantum numbers.

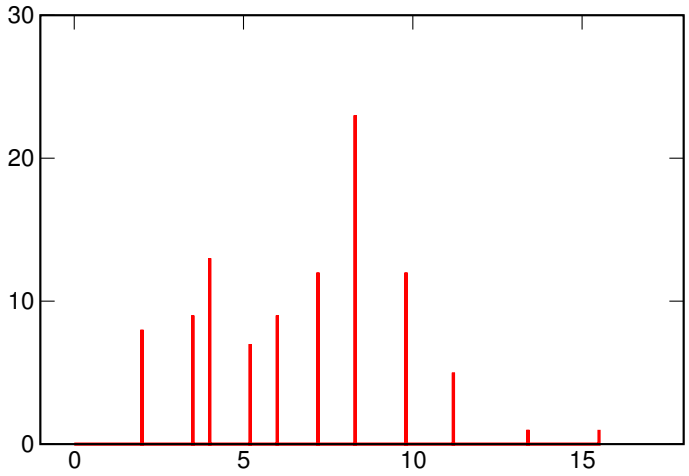

Figure 9: Stripping on ^{48}Cr $\rightarrow$ ^{49}Cr; $0f_{5/2}$ spectroscopic strength.

Acknowledgements Supported by the Ministerio de Educación y Ciencia (Spain), FPA2007-66069, and by the Comunidad de Madrid (Spain), project HEPHACOS P-ESP-00346.

References

[1] M.G. Mayer, Phys. Rev. **75** (1949) 1969; O. Haxel, J.H.D. Jensen, and H.E. Suess, Phys. Rev. **75** (1949) 1776.

[2] V. R. Pandharipande, I. Sick and P. K. A. deWitt Huberts, Rev. Mod. Phys. **69** (1997) 981.

[3] S. Fantoni and V. R. Pandharipande, Nucl. Phys. A **427** (1984) 473.

[4] J. Cavedon *et al.*, Phys. Rev. Lett. **49** (1982) 978.

[5] E. Caurier, G. Martinez-Pinedo, F. Nowacki, A. Poves and A. Zuker, Rev. Mod. Phys. **77** (2005) 427.

[6] M. Dufour and A. P. Zuker, Phys. Rev. C **54** (1996)1641.

[7] S. C. Pieper, K. Varga and R. B. Wiringa, Phys. Rev C **66** (2002) 044310.

[8] P. Navratil and W. E. Ormand, Phys. Rev. Lett. **88** (20022) 152502.

[9] G. Martínez-Pinedo, A. Zuker, A. Poves and E. Caurier, Phys. Rev C **55** (1997) 187.

[10] M. Baranger, Nucl. Phys. A **149** (1970) 225.

[11] L. Gaudefroy *et al.*, Phys. Rev. Lett. **97** (2006) 092501.

[12] L. Gaudefroy *et al.*, Phys. Rev. Lett. **99** (2007) 099202.

[13] A. Signoracci and B. Alex Brown, Phys. Rev. Lett. **99** (2007) 099201.